TECHNISCHE UNIVERSITÄT MÜNCHEN
Klinikum rechts der Isar
Institut für Diagnostische und Interventionelle
Radiologie (Direktor: Prof. Dr. Ernst J. Rummeny)

Cross-Sectional and longitudinal MR-based evaluation of fat depots in subjects with obesity and risk factors for type 2 diabetes mellitus

Christian Cordes

Vollständiger Abdruck der von der Fakultät für Medizin der Technischen Universität München zur Erlangung des akademischen Grades eines
Doktors der Medizin
genehmigten Dissertation.

Vorsitzender: Prof. Dr. Jürgen Schlegel
Prüfer der Dissertation:
1. Prof. Dr. Ernst J. Rummeny
2. Priv.-Doz. Dimitrios Karampinos, Ph.D.

Die Dissertation wurde am 21.02.2018 bei der Technischen Universität München eingereicht und durch die Fakultät für Medizin am 07.11.2018 angenommen.

Table of Content

ABBREVIATIONS

BMD = Bone Mineral Density

BMFF = Bone Marrow Fat Fraction

BMI = Body Mass Index

CT = Computed Tomography

HCC = Hepato Cellular Carcinoma

MHO = Metabolic Healthy Obese

OIR = Obese Insulin Resistant

MR = Magnetic Resonance

MRI = Magnetic Resonance Imaging

MRS = Magnetic Resonance Spectroscopy

NAFLD = Non-Alcoholic Fatty Liver Disease

NASH = Non-Alcoholic Steatohepatitis

NAT = Non-Adipose Tissue

OGTT = Oral Glucose Tolerance Test

PDFF = Proton Density Fat Fraction

PPM = Parts Per Million

PRESS = Point-Resolved Spectroscopy

ROI = Region Of Interest

SAT = Subcutaneous Adipose Tissue

STEAM = Stimulated Echo Acquisition Mode

T2DM = Type 2 Diabetes Mellitus

TE = Echo Time

TR = Repetition Time

VAT = Visceral Adipose Tissue

1 Introduction

1.1 Obesity, metabolic syndrome, diabetes and fatty liver disease

According to the WHO (World Health Organization) "overweight and obesity are defined as abnormal or excessive fat accumulation that may impair health" (World Health Organisation, 2016b). For the classification of obesity and overweight the body mass index (BMI) is a common measure. It is defined by the ratio of the body weight [kg] to height squared [m^2]. With a BMI $\geq$ 25 kg/m^2 people are categorized as overweight, with a BMI $\geq$ 30 kg/m^2 as obese. Within the European Union in 2014, 44.7% of the women and 59.1% of the men are considered as obese or overweight (International Diabetes Federation). In the United States (US) in 2009-2010 even 74% of the men and 64% of the women were obese or overweight (National Institute of Diabetes and Digestive and Kidney Diseases).

The International Diabetes Federation defines the metabolic syndrome as "a cluster of the most dangerous heart attack risk factors: diabetes and prediabetes, abdominal obesity, high cholesterol and high blood pressure" (International Diabetes Federation). It is estimated that 25% of adults in the world suffer from the metabolic syndrome.

Diabetes is a chronic disease, which occurs when the pancreas does not produce enough insulin, or when the body cannot effectively use the insulin it produces. This leads to an increased concentration of glucose in the blood (hyperglycemia). Type 2 Diabetes Mellitus develops from a loss of sensitivity to insulin. It is often caused by overweight or physical inactivity. In 2014, 8.5% of adults were affected by type 2 diabetes mellitus (World Health Organisation, 2016a).

Non-alcoholic fatty liver disease (NAFLD) is defined by a histological fat accumulation > 5% in the liver and can lead to non-alcoholic steatohepatitis (NASH) (World Gastroenterology Organisation, 2012). NASH is a chronic form of liver disease, which is defined by fat accumulation in the liver, absence of alcohol consumption and relevant inflammation (Straub et al., 2010). The main reasons for NASH appear to be insulin resistance, obesity and the metabolic syndrome. NAFLD and NASH are diseases with a strong impact on societies – in the US 27-34% of the general population are suffering from the two diseases (World Gastroenterology Organisation, 2012).

All the above diseases mentioned above could cause further complications, including stroke and cardiovascular diseases, resulting in an increased mortality. Therefore, the above metabolic diseases need to be detected early to initiate adequate therapy and prevent complications.

1.2 Abdominal Fat Compartments

Fat is central to the incidence and progression of obesity, diabetes and fatty liver disease. Fat is primarily stored in adipose tissue. Adipose tissue contains about 80% fat; the remaining components are water, proteins and minerals. It can be divided into different compartments including subcutaneous adipose tissue (SAT), organ surrounding tissue (VAT = visceral adipose tissue) and adipose tissue in bone marrow (Shen et al., 2003). SAT is the fat depot between the dermis and the fascia of the muscles. VAT is fat which is within the inner fascia of the abdominal muscles. Furthermore VAT can also be named after the organ to which it is close (e.g. perirenal adipose tissue)(Shen et al., 2003) . Importantly, VAT is associated with a greater risk for hypertension, impaired glucose tolerance/ insulin resistance and the metabolic syndrome than SAT (Lebovitz et al., 2005; Nakamura et al., 1994; Taksali et al., 2008), especially for women (Fox et al., 2007).

Given the different function and role of the different fat depots, there is a need to quantify the regional body composition to discriminate between different metabolic disease phenotypes. Obesity phenotype could be interpreted as the discrimination between obese subjects with a relatively low cardiovascular risk profile (Metabolic healthy obese = MHO) and subjects with insulin resistance and associated elevated risk profile (Obese-insulin resistant = OIR) (Kantartzis et al., 2011; Taksali et al., 2008). Previous studies have outlined the necessity of differentiating between these phenotypes to adjust (dietary) interventions. Kartanzis et al.(Kantartzis et al., 2011) suggested that MHO individuals do not gain the same benefit from lifestyle interventions (regarding the cardiovascular risk) compared to OIR individuals.

1.3 Bone Marrow Fat

An adipose tissue not yet frequently studied in the context of lifestyle interventions is bone marrow fat. The connection between bone marrow fat fraction (BMFF) and obesity is not as clear as for the other types of tissue. Previous studies have reported that dietary intervention can lead to an increasing BMFF in mice (Baek et al., 2012a; Devlin et al., 2010) and NAFLD correlated with a higher lumbar BMFF in children (Yu et al., 2017). A connection between high BMFF and anorexia nervosa has been observed in humans (M. A. Bredella et al., 2014; M. A. Bredella et al., 2009; Ecklund et al., 2017). A study examined the connection between BMFF and insulin resistance as well as blood fat parameters. They found a positive correlation between BMFF and unsaturation index (independent from the obesity of participating women). In addition, BMFF showed a negative correlation with insulin resistance and a positive correlation with HDL serum levels (Ermetici et al., 2017). BMFF is an interesting field of investigation

because a high BMFF is associated with a low bone mineral density (BMD) leading to osteoporosis (Baum et al., 2012; Cohen et al., 2015; M. Hu et al., 2014). Osteoporosis is a well-known disease with an increased risk of fractures, associated with a reduction of quality of life as well as increased mortality, resulting in immense costs for the health systems (Barcenilla-Wong et al., 2015; Bleibler et al., 2014). In the European Union alone, there are 22 million women and 5.5 million men suffering from osteoporosis with 3.5 million new fragility fractures and a cost of 37 billion Euros (including incident fractures, long-term fracture care and pharmacological prevention) (Hernlund et al., 2013). This underlines the necessity of understanding the association of bone health and obesity.

The present thesis focuses on a cross-sectional study investigating the association of different fat depots and on a longitudinal study investigating the effect of diet on different fat depots.

1.4 Cross-sectional study investigating the association of different fat depots

The purpose of the cross-sectional study was to investigate the associations between the liver fat, VAT, SAT, bone marrow fat and blood parameters (including cholesterol, triglycerides, and blood sugar as well as insulin levels) in prediabetic subjects.

1.5 Longitudinal study investigating the effect of diet on different fat depots

The goals of the longitudinal study were to study changes of the composition and volumes of fat during a high calorie restrictive diet for four weeks in obese women.

2 Background

2.1 Fat Quantification using Magnet Resonance Imaging

In general, there are two main imaging techniques for the determination of VAT and SAT volumes: Magnetic Resonance (MR) imaging and computed tomography (CT). CT is faster and cheaper than MR, but is exposing patients to ionizing radiation. For this reason, MR was used in the present studies.

Fig. 1 shows an example of T1-weighted imaging. It was acquired for whole body fat determination. On T1-weighted images, fat appears brighter than water based tissues. This excellent contrast enables distinguishing between fat, muscles and organs (Donald W. McRobbie, 2006; H. H. Hu et al., 2011).

Chemical shift encoding based water-fat MRI (e.g. Dixon method) is an emerging MR technique to determine fat content and volume. Fig. 2 and Fig. 3 show representative Dixon images of the abdomen. The principle of the used two-point Dixon imaging is to generate in-phase and out-of-phase ("two-point") gradient echo images. The basic assumption is to measure a first in-phase image with a signal which is the sum of the water and fat signal ($S_{ip} = S_w + S_f$). By acquiring an additional second out-of-phase image, which is the difference of the signals mentioned above ($S_{oop} = S_w - S_f$) and solving these equations it is possible to calculate an image separated in water and fat only (Donald W. McRobbie, 2006).

Imaging allows studying the spatial distribution of the fat in contrast to MRS (Magnetic Resonance Spectroscopy).

The reproducibility of vertebral bone marrow fat quantifications from C3 (Cervical vertebral body 3) to L5 (lumbar vertebral body 5) was determined with a deviation of 1.7% for water-fat imaging based technologies (Baum et al., 2016).

Borga et al. (Borga et al., 2015) compared the analysis of VAT and SAT by using the traditional T1-weighted imaging and the established sliceOmatic software with the Dixon method and the AMRA software for image analysis of 23 volunteers (Borga et al., 2015). The AMRA software proved to be much faster (3 vs. 40 minutes of manual intervention). Both methods did not show any statistically significant differences (VAT: $p = 0.077$; SAT: $p = 0.147$); the VAT was 4.73 ± 1.99 l (AMRA, dixon) versus 4.73 ± 1.75 l (sliceOmatic, T1) with a p-value of 0.97. SAT analysis showed similar results for both methods: 10.39 ± 5.38 l (AMRA) and 9.78 ± 5.36 l (sliceOmatic). The 95% limit of agreement was -1.06 to 1.07 for VAT and -0.36 to 1.60 for SAT. They concluded that VAT and SAT can be acquired by the very fast multi-point Dixon protocol.

The liver PDFF determined by water-fat imaging technologies also showed a very good reproducibility (SD ≤ 0.66%) (Baum et al., 2016).

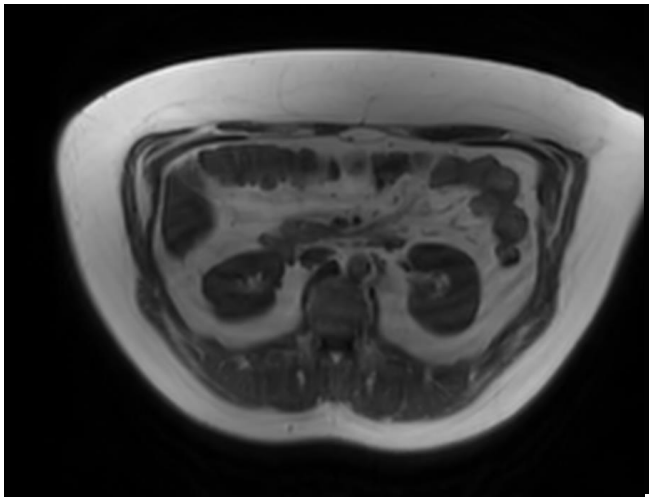

Fig. 1 T1-weighted image which can be used for abdominal fat quantification, positioned supine

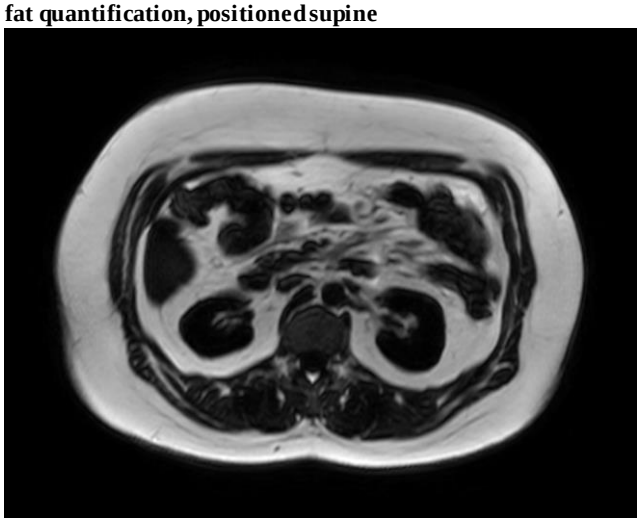

Fig. 2 Fat-only Dixon image

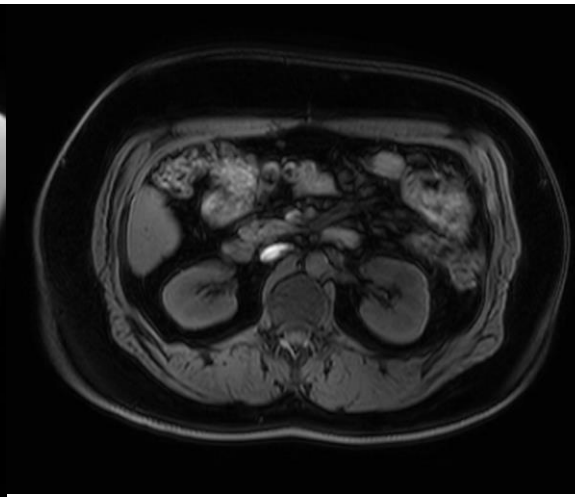

Fig. 3 Water-only Dixon image

2.2 Fat Quantification using Magnetic Resonance spectroscopy (MRS)

Single-voxel spectroscopy allows the determination of fat composition. The underlying measured property in an MRS experiment the chemical shift, which leads to different resonance sequences of fat and water spins as lipids have a lower resonance than water. The water-fat shift is 210/ 420 MHz for 1.5/ 3.0 T. In addition an instant visualization is given, which enables a quality check of the spectroscopy immediately (H. H. Hu et al., 2011).

There are two different main techniques for single-voxel MR spectroscopy: STEAM (Stimulated Echo Acquisition Mode) and PRESS (Point-RESolved Spectroscopy). PRESS

delivers a higher signal to noise ratio, whereas STEAM allows for shorted echo times. The STEAM sequence is based on three selective 90-degree pulses, one in each axis, and generates an echo series, which can be analyzed. The PRESS sequence is based on a spin echo sequence. It generates a signal strength, which is twice as strong as the one from the STEAM sequence. In earlier times PRESS was not able to be operated in as short echo times as STEAM, this problem is now overcome (Donald W. McRobbie, 2006).

MR spectroscopy showed a good reproducibility. Pansini et al. performed a study with 33 healthy volunteers and measured the fat content in several anatomic locations of the hip (femoral head, femoral neck, greater trochanter, proximal femoral diaphysis and acetabulum) with a STEAM sequence twice. They were able to demonstrate a very good reproducibility with correlation between the two measurements of r = 0.90 to 0.98 (Pansini et al., 2012).

Griffith et al. investigated the reproducibility of MRS in order to determine the fat content of the bone marrow of the proximal femur and acetabulum. In 36 subjects, subdivided into groups according to Dual-Energy X-ray Absorptiometry (DXA) results, they examined the fat content with a PRESS sequence twice. They observed a good reproducibility; concordant spectroscopy data were found for all paired measurements in the femoral head, for 92% in the femoral neck and 94% in the femoral shaft. The interclass correlation was 0.85 for the femoral head, 0.78 for the femoral neck and 0.83 for the femoral shaft (Griffith et al., 2009).

For vertebral bodies Li et al. (Li et al., 2011) performed a study in 51 women who were examined from L1 to L4 using a PRESS sequence. Six of them were scanned twice on one day with an average coefficient of variation of 1.7% (range: 1.2 to 2.0%).

The above results demonstrated that MR spectroscopy is a reliable technique.

MR spectroscopy is widely used to measure the PDFF in the liver. It showed a good reproducibility over different field strengths (1.5 T versus 3.0 T). According to a review by Baum et al. (Baum et al., 2016) it has an intra-examination standard deviation of 0.49, whereas the inter-examination standard deviation was 0.46.

The degree of unsaturation is also detectable with MRS. Binggolbali et al. performed saturation level examinations in oil phantoms and volunteers in the spinal bone. They found a good correlation for the STEAM sequence with literature values, better than for the PRESS sequence (Bingolbali et al., 2015).

Lastly, Ruschke et al. recommended PRESS instead of STEAM for unsaturation level measurements in regions where the PDFF is low (Ruschke et al., 2016).

2.3 T2 measurements*

Magnetic fields inhomogeneities are present in MRI measurements because of susceptibility effects. That means there is inhomogeneity caused by air pockets (e.g. in the guts), iron-rich tissues such as in the liver or bone matrix in bone marrow. That affects the relaxation of protons after a radio frequency pulse. The parameter which expresses the inhomogeneity is the T2* relaxation time.

2.4 Postprocessing

2.4.1 Images

After generating the images, post-processing with suitable algorithms is required. Most algorithms work semi-automatically. By using anatomical landmarks, VAT and SAT can be segmented. T1-weighted imaging requires the definition of a binary threshold to classify a voxel as water or fat. To extract fat volumes based on water-fat imaging, the fat-only images are used with a threshold analogous to the T1-based procedure.

2.4.2 Spectra

Based on MRS spectra it is possible to derive fat fractions, e.g. in the liver or bone marrow. By determining integrals belonging to the peaks and putting them in relation to each other, the fat fraction can be computed.

The analysis of spectra can be challenging due to low signal-to-noise ratio or overlapping peaks. Simple integration or simple line fitting are often not able to solve the problems. Another fitting method calculates spectra based on the biochemical composition of the examined tissue frequency using Gaussian-/ Voigt line shapes (Mierisova et al., 2001).

3 Materials and Methods

3.1 Subjects

3.1.1 Cross-sectional study

Inclusion criteria were an age between 18 and 75 and a high risk for T2DM (Type 2 Diabetes Mellitus) according to a screening questionnaire ("Deutscher Diabetes Risiko Test) (Deutsches Institut für Ernährungsforschung Potsdam-Rehbrücke (DIfE), 2014). 35 female and 28 male subjects participated in the study.

Potential subjects went to an initial screening appointment where an oral glucose tolerance test (OGTT), an MR examination for liver fat determination, physical examination, anthropometric measurements and blood samples were obtained. The recruitment was performed at the "Institut für Ernährungsmedizin, Technische Universität München".

According to OGTT and liver fat, subjects were divided into a high and a low risk group.

Exclusion criteria were manifest diabetes, certain endocrinological diseases, chronicle gastrointestinal diseases, psychic diseases, addiction, anti-inflammatory or immunosuppressive therapy, acute or chronicle infectious diseases, cancer, certain liver or biliary disease, kidney insufficiency, anemia, certain clotting disorders and pregnancy (Deutsches Zentrum für Diabetesforschung, 2017; Else Kröner-Fresenius Zentrum für Ernährungsmedizin der Technischen Universität München, 2017).

3.1.2 Longitudinal study

This study was conducted by the Else-Kroener-Fresenius-Center, Institut für Ernährungsmedizin, Technische Universität München and registered on the German Trial Register (DRKS00006210). The patients were recruited by the Else-Kroener-Fresenius-Center. 20 women were included with an age range from 24-65 having a BMI of 34.9 ± 3.8 kg/m^2. Study intervention consisted of four times 200 kcal Modifast meals per day (from Nutrition Sante SAS, Revel, France) and in addition 200 g of vegetables per day for 28 days.

The subjects underwent anthropometric and blood fat value measurements (fasting) and MR one day before and one day after the dietary intervention in a non-fasting state. The analysis of the blood samples was done with an established method by Synlab (Munich, Germany) (Cordes et al., 2015).

3.2 MR examinations

3.2.1 Cross-sectional study

MR examinations were operated on a 3.0 T Philips scanner (Ingenia; Philips Healthcare, Best, Netherlands) with an anterior and posterior coil. Two sets of axial two-point Dixon images were acquired (3D spoiled gradient echo). Scanning parameters were: TR (repetition time) = 4.0 sec., TE (echo time) 1/TE2 = 1.32/ 2.6 msec, flip angle = 10°, bandwidth = 1004 Hz/pixel, 332 x 220 acquisition matrix size, FOV =500 X 446 mm^2, acquisition voxel =1.5 X 2.0 X 5.0 mm^3, 44 slices, parallel imaging using SENSE with a reduction factor r = 2.5. Scan time amounted to 10.6 s and was performed within a single hold of breath. By using the mDixon algorithm on the scanner the water/ fat images were separated.

A six-echo gradient echo sequence (mDixon quant) was used to measure liver- and bone marrow fat fraction and T2* values: TR = 7.8 ms, TE1/ΔTE= 1.3/1.1 ms, flip angle = 3°, bandwidth = 1523 Hz/pixel, 152x133 acquisition matrix size, FOV = 300x403 mm , acquisition voxel = 2.0x3.0x6.0 mm , 25 slices, SENSE with R = 2.2x1.2 (in L/R and F/H respectively).

MR spectroscopy (STEAM) was used for the fat quantification in the liver after acquiring a coronal survey image (Fig. 4). The parameters of the STEAM were as following: TR/ TM = 3500/16 msec, four TE values (in order to perform T2 correction): 10/15/20/25 msec, one dummy scan, one average per TE, 4096 data points, spectral bandwidth = 5 kHz, no water suppression, and no regional saturation bands. This examination lasted 17.5 sec and was performed in a single hold of breath.

For bone marrow fat quantification, a sagittal survey image was acquired from the vertebral column to acquire anatomical information (Fig. 5). A 15 x 15 x 15 mm^3 voxel was placed in the middle of the L5 vertebral body (avoiding degenerated vertebral bodies and the cortical bone) and a STEAM sequence was performed. The parameters of the STEAM sequence were: TR/TM = 6000 /16 msec, four TE values (in order to perform T2 correction) TE = 11/15/20/25 msec, one dummy scan per TE, eight averages per TE (four phase cycles), 4096 data points, spectral bandwidth = 5 kHz, no water suppression and no regional saturation bands. The scan time amounted to 216 sec (Cordes et al., 2015).

Furthermore, STEAM MRS was performed within the SAT and VAT at the level of L5 to determine the level of unsaturation in the abdominal tissues. A 20 x 20 x 20 mm^3 voxel was placed in the according tissue. The scanning parameters were TR = 2.0 s; TE = 11/15/20/25 ms; 4096 samples; spectral bandwidth = 3.5 kHz. 16 averages and the scan time accounted to 136 s.

Fig. 4 Coronal T2 image of the liver, kidneys and spleen in order to plan the liver spectroscopy

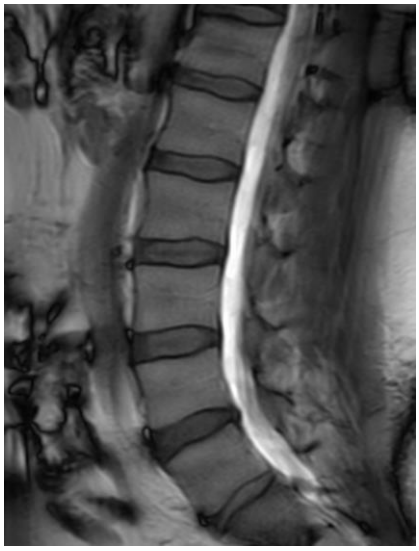

Fig. 5 Sagittal image of the spine in advance of the L5 spectroscopy

3.2.2 Longitudinal study

The longitudinal study was performed using a 3.0 T MR scanner (Ingenia; Philips Healthcare, Best, Netherlands) using anterior and posterior coil. Axial water-fat images of the abdomen and pelvis were acquired using the same mDixon sequence as in the cross-sectional study. Spectroscopy was performed in the liver, L5, SAT and VAT. Scan parameters were identical to those mentioned above in the cross-sectional study part.

3.3 Data analysis

3.3.1 Cross-sectional study

3.3.1.1 SAT/ VAT Segmentation

For the SAT- and VAT- analysis an in-house written semi-automatic algorithm was used. First k-means clustering was used to find similar features (k = 3) in the whole image. The voxels were than divided into three categories (Fig. 6): air/ bone (= no MR signal; light blue); adipose tissue (red (SAT) or yellow (VAT)) and non-adipose tissue (NAT; high water signal; dark blue). Second, isolated voxels were deleted from the mask, as were interior voxels, to leave only the outer boundary as skin contour. After this process, the inner SAT (red) border needed to be found. This was done by removing adipose tissue with a gradient vector flow. The outer SAT border was defined as the border of the whole mask. The VAT compartment (yellow) was defined as adipose tissue within the inner SAT border.

The algorithm required manual corrections. The average manual correction time was 11 minutes for a stack of 44 images. To have a standardized, comparable value, a region from L3 (lumbar vertebral body 3) and twelve stacks above was defined. SAT and VAT ratios were calculated ($SAT\ ratio = \frac{SAT}{SAT+VAT+NAT}$; $VAT\ ratio = \frac{VAT}{VAT+SAT+NAT}$). Normalized SAT and VAT ratios were defined by using anatomical landmarks: from the region directly under the heart up to the top of the femoral heads.

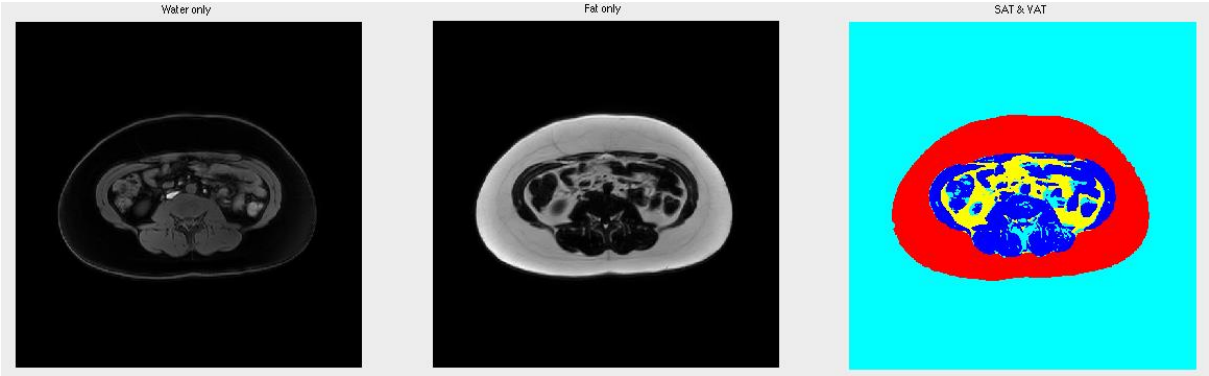

Fig. 6 Images for VAT and SAT segmentation, Water and fat images on the left; processed images on the right (VAT=red, SAT=yellow, Water=dark blue, air=light blue)

3.3.1.2 Spectra analysis of the liver

For the spectra analysis an in-house built algorithm based on MatLab (MathWorks, Natick, MA) was used. A typically measured spectrum is characterized by peaks at 0.9, 1.30, 1.59, 2.00, 2.25, 2.77, 4.2, 5.19 and 5.31 ppm.0.9 ppm:(-$(CH_2)_n$-C**H**$_3$); 2.77 ppm:(–CH=CH-C**H**$_2$-CH=CHab-); 4.2 ppm:(-C**H**$_2$-O-CO-); 2.0 ppm: (-C**H**$_2$-CH=CH-CH_2-), 5.19 ppm: (-C**H**-O-CO-) and 5.31ppm: (-C**H**=C**H**-). It is exemplarily displayed in Fig. 7.

Joint fitting was necessary to further process the spectra based on the different TE acquired data fitting into a signal model with T2 decay effects. The peak fitting was performed on all spectra according to linewidth, peak localization and areas / T2 relaxation time. The result was a proton density fat fraction based on all fat peaks.

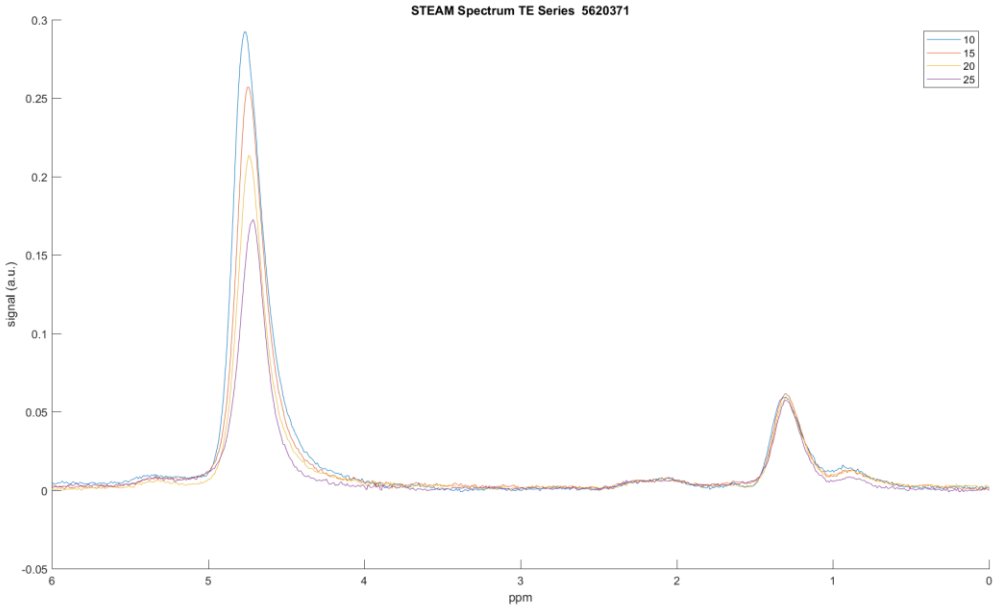

Fig. 7 Representative STEAM spectroscopy of the liver in a subject with a high liver fat content (10.97%) at four different echo times. The right smaller peak represents the fat, the high peak at about 5 ppm the water peak.

3.3.1.3 Spectra Analysis of the Bone marrow

A broad water peak is present in the bone marrow, overlapping with fat peaks. To solve this problem a peak fitting was performed by constraining peaks at 4.2 ppm and 5.19 ppm at a certain peak ratio at 0.9 ppm and 1.30 ppm, based on previously known triglyceride structure. An example of a spectrum measured is shown in Fig. 8.

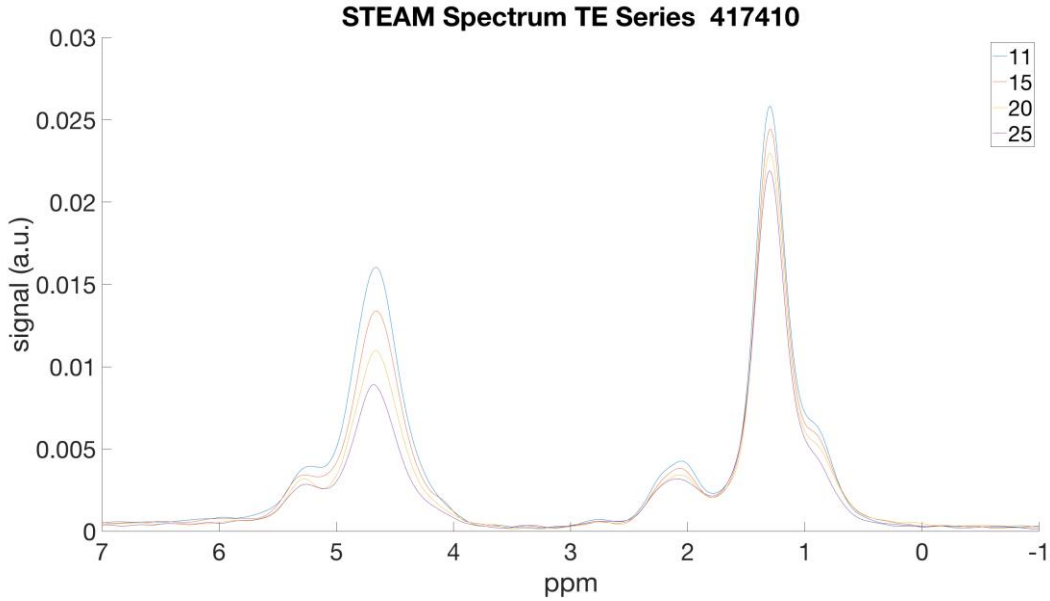

Fig. 8 Representative spectra of the bone marrow at four different echo times with the fat peak (left) and the water peak (right); spectra analysis from MATLAB.

*3.3.1.*4 SAT/VAT unsaturation

Spectra of the first TE were processed using a frequency based fitting routine. Olefinic fatty acids were represented in peak A, the methylene fatty acids in peak F (Fig. 9). To determine the unsaturation of the VAT or SAT the ratio of $\frac{F}{A}$ was used.

The MR spectra at the first TE were processed offline using custom-built frequency-based peak fitting routines. The area of the olefinic peak (peak A in Fig. 9) and the methylene peak (peak F in Fig. 14) were computed and the ratio of the olefinic peak to the methylene peak (ratio F to A) was determined as a measure of fat unsaturation in SAT and VAT.

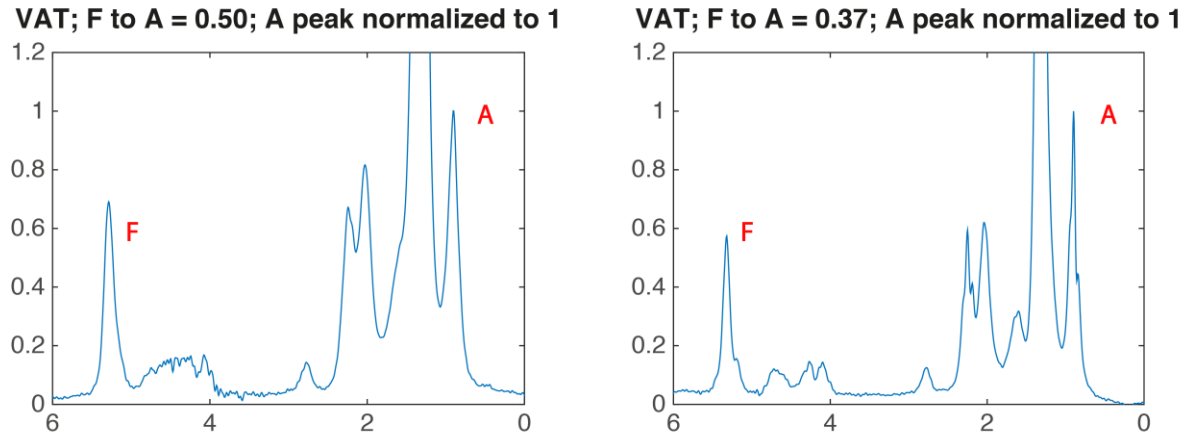

Fig. 9 MR spectra of two subjects with different ratios of unsaturated to saturated fatty acids in the VAT

3.3.1.5 Liver fat fraction / T2 values*

Based on the mDixon images the fat content in the liver and T2* values were computed. The proton density fat fraction map (PDFF) in the liver was calculated online on the scanner using the mDixon quant algorithm.

The liver fat fraction and T2* values were measured in segment VII (Rummeny et al., 2006), its size was 3 cm^2. The acquired image series was opened in Osirix (Pixmeo SARL, Geneva, Switzerland), which consisted of fat images, a fat fraction map, water images, B0 images and T2* images. Afterwards mean fat fraction and T2* values from the exact same position were exported (Fig. 10, Fig. 11).

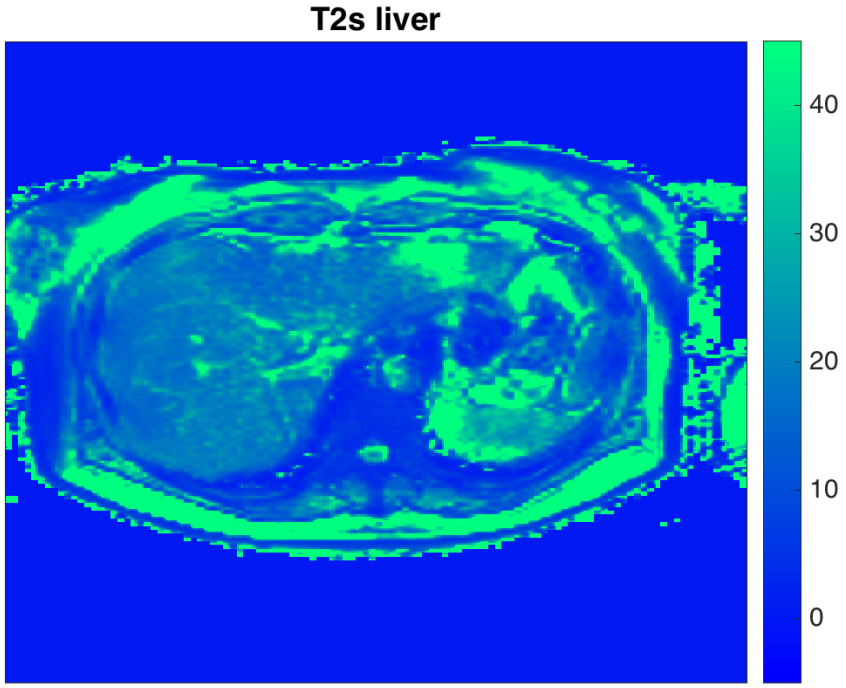

Fig. 10 Representative T2* map of the liver [ms]

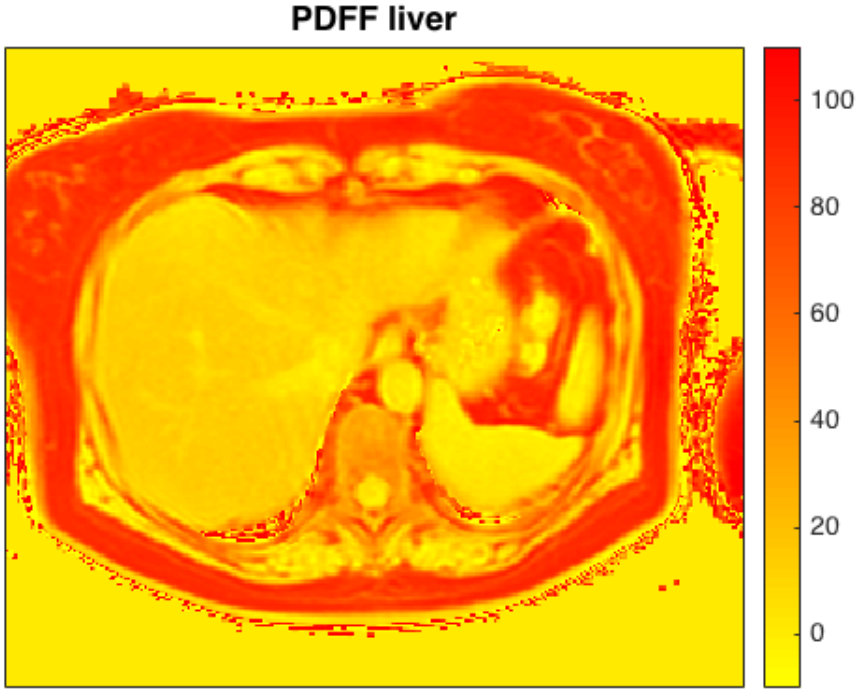

Fig. 11 Representative Fat fraction map of the liver [%]

3.3.1.6 Bone marrow fat fraction / T2 values*

The procedure from the liver fat analysis was applied in a similar way to the bone marrow, as reported in 3.3.1.5. The online reconstruction algorithm (mDixon quant) on the scanner was

used. The post processing was done using Osirix. First the most central slice (greatest diameter of the spinal canal / processi spinosi completely visible) was determined. Then ROIs were placed on the anterior part of the vertebral bodies avoiding the cortex in the vertebral body from L1 (lumbar vertebral body 1) to L5. Lastly, mean fat fraction values and T2* values were determined in each lumbar vertebral body (Fig. 12, Fig. 13).

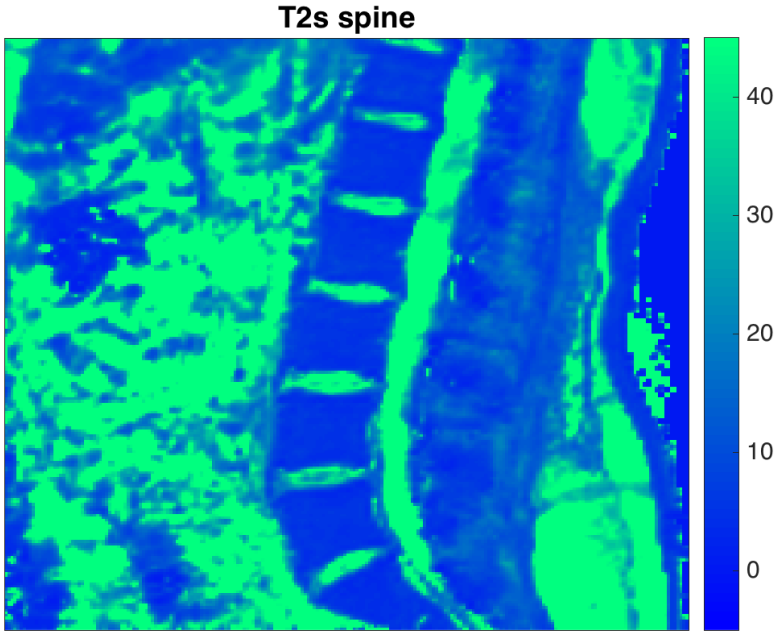

Fig. 12 Representative T2* map of the spine [ms]

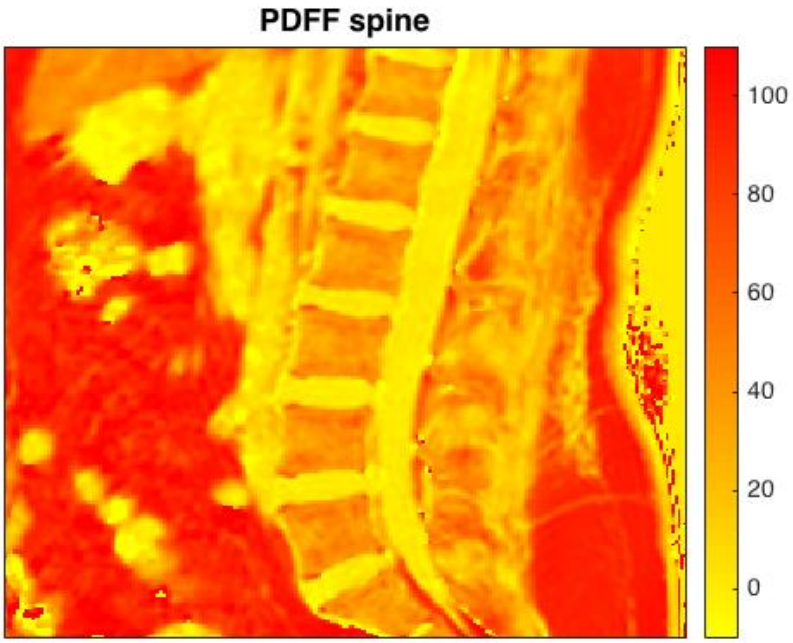

Fig. 13 Representative Fat fraction map of the spine [%]

3.3.1.7 Blood values and anthropometric measurements

Parameters for the body composition weight, height and BMI, the waist- and hip circumference, the percentage body fat content, the fat- and lean mass were measured. Oral glucose tolerance test was performed measuring the glucose concentration and insulin levels fasting and 30, 60, 90 and 120 minutes after consuming 75g of glucose. HbA1c cholesterol and triglycerides values were measured. Blood value and anthropometric measurements were performed by an external laboratory and the "Institut für Ernährungsmedizin", respectively.

3.3.2 Longitudinal study

The SAT- / VAT- segmentation from the data of the longitudinal study was similar to the method for the cross-sectional study mentioned in 3.3.1.1. However, only the slices from the level of L3 and 12 slices above were analyzed.

Spectra were analyzed as reported in the cross-sectional study section.

3.4 Statistical analysis

3.4.1 Cross-sectional study

The statistical analyses were performed using SPSS (Chicago, IL). A Shapiro-Wilk Test was performed to check normal distribution of the measured parameters. Differences between male and female subjects were analyzed using the Mann-Whitney-U test because parameters were not normally distributed. A two-sided 0.05 level of significance was used. Correlations were computed using Spearman correlation coefficient.

3.4.2 Longitudinal study

For the statistical analysis SPSS (Chicago, IL) was used. A two-sided 0.05 level of significance was used. Most parameters were normally distributed, according to Shapiro-Wilk test. Due to normal distribution the two points of time were compared with paired student's t-tests. The results are shown with mean and standard deviation. BMFF and serum lipids at baseline, BMFF and serum lipids at follow-up and follow-up BMFF and baseline serum lipids were correlated. To examine the relationship between SAT, VAT, NAT volumes und ratios at baseline and bone marrow fat changes, linear regression was performed.

4 Results

4.1 Cross-sectional study

The data analysis of the pre-diabetic study included 63 baseline subjects.

4.1.1 Explorative data analyses

Tab. 1 summarizes the metabolic parameters (35 female, 28 male). The average BMI was 30.91 kg/m^2; 31 subjects were obese (BMI > 30kg/m^2), 21 overweight (BMI > 25kg/m^2 < 30 kg/m^2) and four subjects had normal weight (BMI < 25 kg/m^2).

The average level of fasting glucose was 104.45 mg/dl. At baseline, nine of the subjects were non-diabetic (fasting glucose <100mg/dl), 41 in the impaired fasting glucose tolerance range (BG 100-125 mg/dl) and one diabetic with a fasting glucose of 133 mg/dl (which must be confirmed at a second point of time to have diabetic status).

The mean TG concentration was 137.29 mg/dl, and the mean cholesterol was within the normal range (219.54 mg/dl).

A liver fat fraction higher than 5% is classified as steatohepatitis. Twelve of the eighteen cross-sectional study patients who underwent the liver fat analysis had steatohepatitis (11.64% ± 10.62%).

4.1.2 Differences between male and female subjects

SAT volume, BMI and bone marrow-fat and liver fat were not significantly different, VAT volume ($p = 0.0032$) was greater in males than females (Table 2).

4.1.3 Correlations

4.1.3.1 Dixon-based Liver fat fraction

Correlations with the liver fat are shown in Tab. 3. A strong positive correlation was found between the Dixon-based liver fat fraction and the Insulin levels (0: $r = 0.664$, $p = 0.002$; 30: $r = 0.612$, $p = 0.005$) as well as the insulinogenic index ($r= 0.691$, $p = 0.001$).

Moderate correlations with the liver fat fraction were calculated for SAT ($r = 0.505$, $p = 0.009$) and VAT volumes ($r = 0.395$, $p = 0.046$), the weight ($r = 0.390$, $p = 0.049$) and the hip circumference ($r = 0.427$, $p = 0.042$). The Matsuda index correlated strongly negative with the liver fat ($r = -0.696$, $p = 0.001$) and the SAT unsaturation moderately negative ($r = 0.530$, $p < 0.05$). The correlation between the unsaturation of SAT and liver fat is exemplarily displayed in Fig. 14 ($r = -0.53$, $p = 0.02$, Tab. 3).

4.1.3.2 VAT volumes

VAT volumes showed correlations with several parameters as displayed in Tab. 4. It correlated positively with the SAT volume in the same range ($r = 0.414$, $p = 0.001$), the height ($r = 0.533$, $p < 0.001$), the weight ($r = 0.702$, $p < 0.001$), the waist ($r = 0.747$, $p < 0.001$) and the hip circumference ($r = 0.387$, $p = 0.002$). Serum cholesterol ($r = -0.284$, $p = 0.041$), HDL ($r = -0.469$, $p < 0.001$) and the Matsuda ($r = -0.303$, $p = 0.045$) index showed a negative association with the VAT.

4.1.3.3 SAT volumes

The SAT volume in the same range as the VAT volume showed strong positive correlations on a high significant level with the fat mass ($r = 0.861$, $p < 0.001$), the BMI ($r = 0.827$; $p < 0.001$), the hip circumference ($r = 0.806$; $p < 0.001$), the waist circumference ($r = 0.707$; $p < 0.001$) and the weight ($r = 0.650$; $p < 0.001$) (Tab. 5). Whereas the insulin levels from the OGTT correlated moderately positive (0 min: $r = 0.486$, $p = 0.001$; 30 min: $r = 0.479$, $p = 0.001$; 60 min: $r = 0.465$, $p = 0.001$). Triglyceride blood levels showed a weak correlation with the SAT volume ($r = 0.319$, $p = 0.021$).

Moderate negative correlations were found for SAT volume and the Matsuda index ($r = -0.516$, $p < 0.001$), F to A fat level in SAT ($r = -0.396$, $p = 0.006$) and F to A fat level in VAT ($r = -0.368$, $p = 0.001$) (Tab. 5).

4.1.3.4 Bone marrow fat fraction

MRS-based bone marrow fat fractions showed a positive correlation with the Dixon-based bone marrow fat fraction from L1 to L5 (based on the Dixon images; $r = 0.560$ to 0.767; $p < 0.004$). Body weight ($r = -0.338$, $p = 0.007$), BMI ($r = -0.360$, $p = 0.004$) and hip circumference ($r = -0.308$, $p = 0.018$) showed a negative correlation with MRS-based bone marrow fat fraction.

	Liver ff	L 5 ff spectro	Unsat SAT	Unsat VAT	Mean ff L5 *	Mean ff L4*	Mean ff L3*	Mean ff L2*	Mean ff L1*	Height [cm]	Weight [kg]	BMI [kg/m2]
Mean	11.64	0.48	0.47	0.52	38.31	38.55	41.10	42.90	43.23	170.87	90.55	30.91
SD	10.62	0.10	0.16	0.12	10.43	10.83	11.89	12.06	12.37	11.01	17.87	4.93
N	34	80	40	40	33	32	33	33	33	80	81	80
	Waist [cm]	**Hip [cm]**	**Fat %**	**Fat mass [kg]**	**Lean mass [kg]**	**BZ0 [mg/dl]**	**BZ30 [mg/dl]**	**BZ60 [mg/dl]**	**BZ90 [mg/dl]**	**BZ120 [mg/dl]**	**Ins 0**	**Ins 30**
Mean	105.36	110.88	35.36	32.06	58.21	104.45	187.72	184.42	143.64	114.77	110.39	759.60
SD	12.25	11.31	8.94	11.21	13.71	12.29	29.10	46.27	33.88	33.45	58.22	497.12
N	78	78	78	78	78	76	76	76	76	76	72	72
	Ins 60	**Ins 90**	**Ins 120**	**HBA1C [%]**	**CHOMG [mg/dl]**	**TGMG [mg/dl]**	**HDLMG [mg/dl]**	**LDLMG [mg/dl]**	**Matsuda**	**Insulinogenic Index**	**Dispositions Index**	
Mean	1089.47	1019.03	710.46	5.88	219.54	137.29	54.44	142.05	7.36	144.81	820.38	
SD	638.04	778.93	666.80	0.39	36.27	68.27	12.67	31.09	4.73	126.94	519.81	
N	72	72	72	80	80	80	80	80	72	72	72	

Tab. 1 Mean values and standard deviation of parameters measured in the cross-sectional study part; *=based on mDixon images

	BMI [Kg/m^2]	**VAT volume** [mm^3]	**SAT volume** [mm^3]	**Liver fat fraction** [%]	**L5 fat fraction** [%]
Mean ± SD Male	31 ± 4.3	5970692 ± 2587941	9048572 ± 3589932	11.85 ± 11.19	47.30 ± 9.05
Mean ± SD female	31 ± 5.30	3913365 ± 1680187.915	10953031 ± 3768097	10.86 ± 9.78	48.21 ± 10.48
p	0.8154	0.0032	0.1015	0.7659	0.4614

Tab. 2 Differences in males and females of the cross-sectional study part

Liver fat fraction vs.	**Total VAT**	**Total SAT**	**Weight**	**BMI**	**Hip**	**Ins 0**	**Ins 30**	**Ins 60**	**Ins 90**	**Ins 120**	**Matsuda**	**Insul. Index**	**F to A SAT**
n	26	26	26	25	23	19	19	19	19	19	19	19	23
r	0.395	0.505	0.390	0.411	0.427	0.664	0.793	0.612	0.500	0.446	-0.696	0.691	-0.530
p	0.046	0.009	0.049	0.041	0.042	0.002	0.000	0.005	0.029	0.056	0.001	0.001	0.02

Tab. 3 Correlation of the Dixon-based liver fat fraction in the cross-sectional study part

VAT vs.	SAT	Height	Weight	Waist	Hip	Ins 0	Cho	HDL	Matsuda
n	63	62	63	60	60	44	52	52	44
r	0.414	0.533	0.702	0.747	0.387	0.390	-0.284	-0.469	-0.303
p	0.001	0.000	0.000	0.000	0.002	0.009	0.041	0.000	0.045

Tab. 4 Correlations of the VAT volume in the cross-sectional study part

SAT vs.	L5 ff	Weight	BMI	Waist	Hip	Fat mass	Ins 0	Ins 30	Ins 60	Ins 90	Ins 120	TG	Matsuda	Insulinog. Index
n	62	63	62	60	60	60	44	44	44	44	44	52	44	44
r	-0.306	0.650	0.827	0.707	0.806	0.861	0.486	0.479	0.465	0.342	n.s.	0.319	-0.516	0.345
p	0.015	0.000	0.000	0.000	0.000	0.000	0.001	0.001	0.001	0.023	n.s.	0.021	0.000	0.022

Tab. 5 Correlations of the SAT volume with other parameter in the cross-sectional study part

BMFF vs.	L5 ff*	L4 ff*	L3 ff*	L2 ff*	L1 ff*	Weight	BMI	Hip
n	27	26	27	27	27	62	61	59
r	0.697	0.560	0.767	0.698	0.736	-0.338	-0.360	-0.308
p	0.000	0.003	0.000	0.000	0.000	0.007	0.004	0.018

Tab. 6 Correlations of the MRS-based BMFF in the cross sectional study part, *=based on the Dixon images

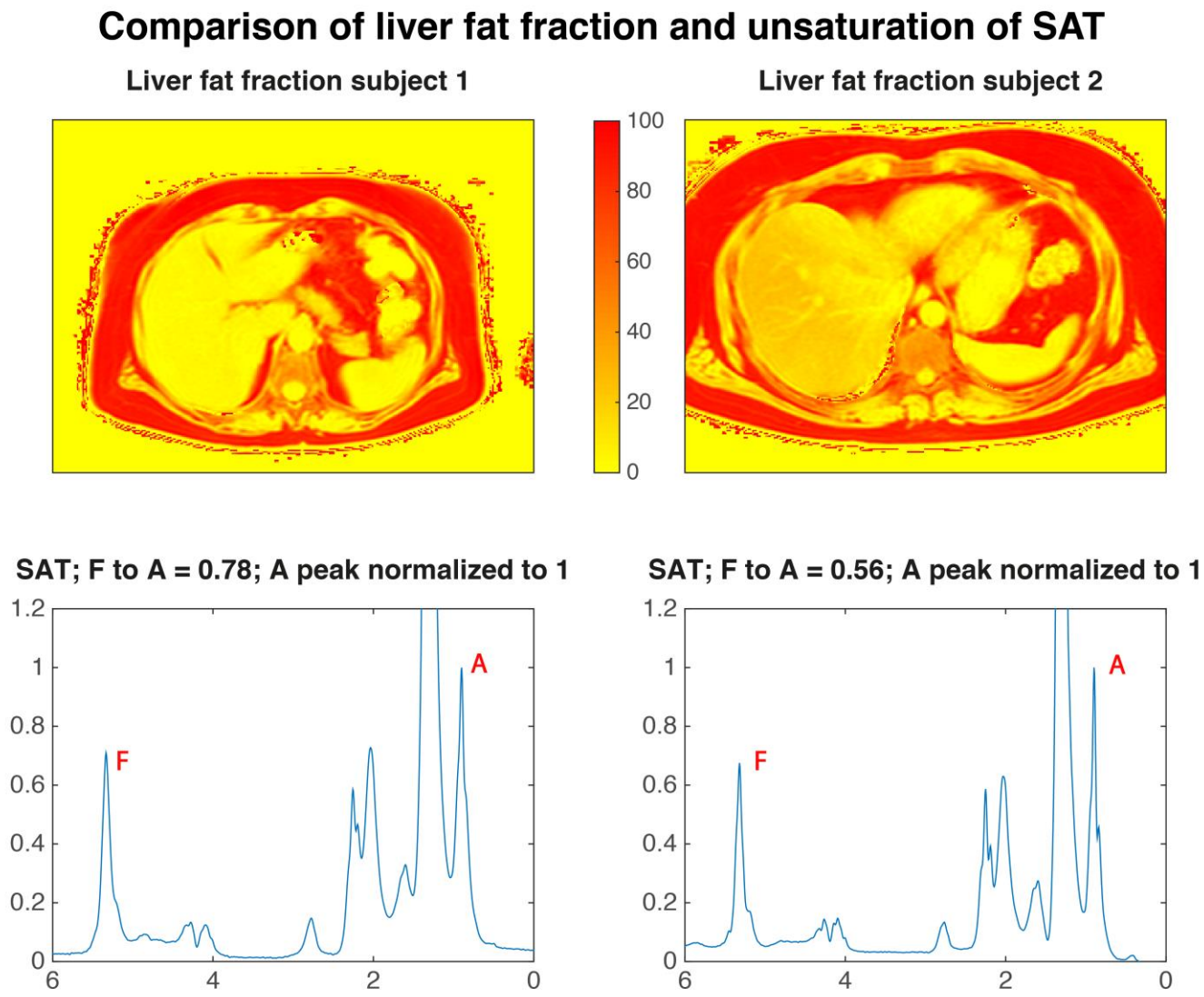

Fig. 14 A Subject with a high liver fat fraction shows a low unsaturation level in the subcutaneous fat

4.2 Longitudinal study part

4.2.1 MR-assessed Fat depots changes

According to Tab. 7 mean weight loss was 7.2 ± 1.6 % ($p < 0.001$) and absolute weight loss 6.9 ± 1.8 kg. BMI decreased by 7.0 ± 1.8 % ($p < 0.001$), and 2.5 ± 0.7 kg/m^2 in absolute values, respectively. Similarly, liver fat fraction showed a decrease of 40 ± 23.5 % ($p < 0.001$). After the intervention, the SAT and VAT volumes decreased significantly by 8.5 ± 4.4 % (SAT) and 15.1 ± 8.7 % (VAT), respectively. Changes in the NAT were not significant ($p = 0.20$), as were no significant changes in the BMFF detected (-1.1 ± 8.2%, $p = 0.39$).

4.2.2 Blood samples

Blood fat values changed significantly after the intervention (Tab. 7). The total cholesterol level showed a significant reduction by 14.2 ± 9.7 % ($p < 0.0001$), the triglycerides by 12.6 ± 23.5 % ($p = 0.035$), the LDL by 14.3 ± 12.9 % ($p < 0.001$), while the HDL level increased by 14.5

± 10.7 %.

4.2.3 Connections between BMFF and Serum lipids

A positive association for the blood cholesterol level and the BMFF before the intervention (r = 0.489; p = 0.029) was detected, as well as for the baseline cholesterol and follow up BMFF (r = 0.547; p = 0.013). Subsequent analyses of the cholesterol level showed a correlation for LDL (r = 0.473, p = 0.035) and HDL/LDL ratio (r = 0.510; p = 0.021) with the baseline BMFF (Tab. 8).

Neither statistically significant changes between follow-up BMFF and follow-up serum lipid values nor for HDL and triglycerides with the BMFF at baseline or follow-up were observed.

4.2.4 Connections between BMFF changes and abdominal tissue distribution

BMFF changes varied among the scanned subjects – reductions in 13 subjects and increases in seven participants. However, the changes in the BMFF were not correlated statistically significant with the weight reduction, blood fat values or the above mentioned fat depot changes. Baseline abdominal tissue distribution and absolute BMFF changes were significant for SAT (r = 0.489; p = 0.029) and NAT (r = -0.493; p = 0.027) (Tab. 9).

Furthermore, relative changes of the BMFF were associated with baseline abdominal tissue distribution, SAT ratio ($\frac{SAT}{SAT+VAT+NAT}$) , r = 0.579; p = 0.008, VAT ratio ,r = -0.453; p = 0.045, and NAT ratio, r = -0.530; p = 0.016.

	before diet	after diet	Relative change (%)	p-value
age (y)	47.0 ± 11.4			
weight (kg)	95.1 ± 13.4	88.2 ± 12.3	-7.2 ± 1.6	<0.001
BMI (kg/m^2)	34.9 ± 3.8	32.5 ± 3.5	-7.0 ± 1.8	<0.001
BMFF (%)	43.1 ± 12.1	42.5± 12.2	-1.1 ± 8.2	0.39
Liver fat fraction (%)	10.3 ± 8.3	5.5 ± 5.1	-40.3 ± 23.5	<0.001
SAT[1] volume (cm^3)	2459 ± 800	2248 ± 739	-8.5 ± 4.4	<0.001
VAT volume (cm^3)	918 ± 261	780 ± 238	-15.1 ± 8.7	<0.001
NAT volume (cm^3)	1651 ± 240	1619 ± 237	-1.7 ± 6.8	0.20
SAT ratio (%)	48.1 ± 10.3	47.6 ± 9.9	-0.9 ± 3.5	0.20
VAT ratio (%)	18.4 ± 5.2	16.9 ± 4.9	-8.2 ± 7.5	<0.001
NAT ratio (%)	33.5 ± 6.8	35.6 ± 7.1	6.4 ± 6.3	<0.001
cholesterol (mg/dl)	191 ± 39	162 ± 29	-14.2 ± 9.7	<0.001
triglycerides (mg/dl)	121 ± 64	98 ± 48	-12.6 ± 23.5	0.035
LDL (mg/dl)	118 ± 37	100 ± 26	-14.3 ± 12.9	<0.001
HDL (mg/dl)	52 ± 9	44 ± 9	-14.5 ± 10.7	<0.001
LDL/HDL (-)	2.36 ± 0.78	2.33 ± 0.69	0.6 ± 16.5	0.68

Tab. 7 Overview over the most important changes of anthropometric, MR detected fat depots and blood value changes in the longitudinal study part

	BMFF before diet vs	BMFF after diet vs
cholesterol (mg/dl) before diet	0.489 (p = 0.029)	0.547 (p = 0.013)
LDL (mg/dl) before diet	0.473 (p = 0.035)	0.543 (p = 0.013)
LDL/HDL (-) before diet	0.511 (p = 0.021)	0.510 (p = 0.021)

Tab. 8 BMFF correlations before and after the dietary intervention with serum lipid values

	BMFF absolute difference (%)	BMFF relative difference (%)
SAT volume (cm^3) before diet	0.489 (p = 0.029)	0.489 (p = 0.029)
VAT volume (cm^3) before diet	n.s.	n.s.
NAT volume (cm^3) before diet	-0.493 (p = 0.027)	-0.532 (p = 0.016)
SAT ratio (%) before diet	0.536 (p = 0.015)	0.579 (p = 0.008)
VAT ratio (%) before diet	n.s.	-0.453 (p = 0.045)
NAT ratio (%) before diet	-0.539 (p = 0.014)	-0.530 (p = 0.016)

Tab. 9 BMFF difference correlation with adipose tissue volumes and ratios before and after the intervention

5 Discussion

5.1 Cross-sectional study part

The cross-sectional study investigated the association of different adipose tissues and possible gender-related differences.

A positive correlation of the liver fat with VAT ($r = 0.395$, $p = 0.046$), SAT ($r = 0.505$, $p = 0.009$), BMI ($r = 0.411$, $p = 0.041$) and hip circumference ($r = 0.427$, $p = 0.041$) was observed, consistent with the literature. Kotronen et al. performed a study on 70 diabetic and 70 non-diabetic subjects (Kotronen et al., 2008) and observed a positive correlation of the liver fat with BMI. A stronger correlation between liver fat and BMI was found in diabetic subjects ($r = 0.45$, $p < 0.0001$) than in non-diabetic ($r = 0.26$, $p = 0.029$). In their study, waist circumference correlated with liver fat stronger for diabetic ($r = 0.45$, $p = 0.0001$) than for non-diabetic subjects ($r = 0.29$, $p = 0.017$). VAT correlated with liver fat in diabetic and non-diabetic subjects ($r = 0.45$, $p < 0.0001$), whereas they did not find any correlations of liver fat with SAT.

Significant associations of the liver fat fraction with insulin levels (fasting insulin: $r = 0.663$, $p = 0.002$) from the oral glucose tolerance test, the insulinogenic index ($r = 0.691$, $r = 0.001$) and negative with the Matsuda index ($r = -0.696$, $p = 0.001$) were observed.

The study from Kotronen et al., mentioned above, reported a positive connection with fasting insulin- ($r = 0.55$, $p < 0.0001$) and fasting glucose blood level ($r = 0.29$, $p = 0.0006$), which was not observed in our study.

In a study with 22 healthy patients and 207 suffering from NAFLD, designed and operated by Lomonaco et al. (Lomonaco et al., 2012), they detected a higher hepatic and muscular insulin resistance in patients with NAFLD compared to healthy subjects (fasting plasma insulin in obese without NAFLD 3.8 ± 0.5 µU/l vs 14.3 ± 0.7 µU/l in patients with NAFLD).

The association of the liver fat fraction with the unsaturation profile of the SAT is noteworthy. These results suggest that abdominal tissue dysfunction is associated with the clinically relevant liver fat, which could be a future point of risk stratification. Machann et al. (Machann et al., 2013) reported a negative association for VAT volume and unsaturation, whereas Lundbom et al. (Lundbom et al., 2011) found a good correlation between unsaturation of the liver fat and unsaturation of the SAT ($r = 0.837$) and VAT ($r = 0.879$) in 16 subjects with a high liver fat fraction (> 5%). They did not find connections between quantified liver fat and unsaturation in SAT or VAT. They also reported a correlation between SAT volume and unsaturation ($r = -0.662$) and VAT volume and SAT unsaturation ($r = 0.611$). This could be interpreted as a higher VAT volume, which is generally regarded as unhealthy and is associated with a lower

unsaturation level. As those studies and our work were performed in a relatively small sample size, it should be studied more thoroughly in the future.

When comparing VAT, SAT volume, liver and bone marrow fat between males and females a statistically significant difference was demonstrated only for the VAT volume, whereas previous studies reported also a higher SAT in men than in women (Lemieux et al., 1993; Schreiner et al., 1996).

Similarly, Westerbacka et al. (Westerbacka et al., 2004) reported that in a group of 132 participants (male and female equally numbered, female with a higher BMI) liver fat values were not statistically significant different between men and women in that study.

MRS-based BMFF of L5 was associated with the water/fat imaging based bone marrow fat fractions of the spine (L1 to L5). This finding demonstrated the validity of water-fat imaging as reported previously (Ojanen et al., 2014; Shen et al., 2013). Shen et al. (Shen et al., 2013) found a similar correlation ($r = 0.78$) for the fat fraction in the L3 vertebral body measured by MRS and mDixon based techniques.

The fat fraction in L5 was not different between men and women. This may be due to the relatively small sample size as a previous study with 154 participants (Kugel et al., 2001) observed a higher fat fraction in men compared to women.

5.2 Longitudinal study

The results from the longitudinal study allowed further insights into interventional changes of abdominal fat depots, liver and bone marrow fat. With the applied diet, it was possible to improve the blood fat profile significantly, as well as the liver fat content. However, the BMFF did not decrease significantly: seven subjects showed an increase and thirteen a decrease, which was correlated to the abdominal tissue distribution at baseline. In general the detected changes in the BMFF (range: 6.1-6.6%) were much smaller than in the other fat depots.

The liver fat could be reduced by the amount as reported in similar studies performed in men (Cowin et al., 2008; Vitola et al., 2009). In consistency with a previous study, a higher VAT loss than SAT was observed here (Chaston et al., 2008). The finding that serum lipids and bone marrow fat are associated is in line with previous studies (Miriam A Bredella et al., 2013; Sadie-Van Gijsen et al., 2013).

A positive correlation of BMFF at baseline with the total cholesterol level, LDL and LDL/HDL ratio at the follow-up measurements was observed. In consistency, previous studies observed a positive correlation between BMFF and serum lipids (Miriam A Bredella et al., 2013; Sadie-Van Gijsen et al., 2013).

A previous study demonstrated a positive correlation between BMFF and HDL cholesterol level

(Ermetici et al., 2017). However, obese and non-obese women participated and were not discriminated in this study.

Changes in BMFF have been previously investigated. In an animal studies an increase of the BMFF was found during starvation (Baek et al., 2012b; Devlin et al., 2010), as well as for patients with anorexia nervosa (M. A. Bredella et al., 2014; M. A. Bredella et al., 2009). However, further studies reported converse results: Westphal et al. found a decrease in the bone marrow fat by 3.5% induced by a weight loss of 9.2 kg (Bosy‐Westphal et al., 2011). Shen et al. did not observe any significant changes in the BMFF after weight loss (Shen W, 2007). Schafer et al. examined the bone marrow fat content before and after surgery in patients who underwent bariatric surgery. They found a mean BMFF decrease by 7.5% ($p= 0.05$) for diabetic subjects and an increase by 0.9% ($p= 0.84$) for non-diabetic subjects.

Due to these conflicting results, subsequent analyses were performed. The BMFF decrease did not correlate significantly with the changes of SAT, VAT or liver fat and serum lipids. However, the distribution of fat before the intervention was associated with bone marrow fat changes: a high SAT volume at baseline led to a rise of the BMFF, whereas a high NAT and VAT ratio were connected with a loss of bone marrow fat. Several studies (Baum et al., 2012; M. A. Bredella et al., 2011; Cohen et al., 2015; Griffith et al., 2005; Griffith et al., 2006; Karampinos et al., 2015; Kim et al., 2017; Paccou et al., 2015; Schafer et al., 2015; Shen W, 2007; Wren et al., 2011; Yeung et al., 2005) showed that bone mineral density is negatively associated with bone marrow fat. Therefore, the authors hypothesized that high intensive calorie restriction in a short period could be harmful for bone health.

Dietary interventions have been shown to have a dramatic effect on liver fat. A review from Thoma et al. (Thoma et al., 2012) evaluated the influence of dietary interventions on the NAFLD. The type of intervention was either diet only, exercise-only or a combination of both. A dietary intervention for the duration of one to six months led to an absolute reduction of the liver fat by 4-10% (relative reduction 42-81%). Two exercise-only interventions measured after a four-week duration, an absolute reduction of 1.8 % in the liver fat (relative reduction 21%); a further study focused on the liver enzymes ALT and AST and found a reduction by 47/48%. Seven studies combined exercise and diet over 3 to 12 months and reported an absolute reduction of 2-4.6% of the liver fat (relative 13-51%).

5.3.Limitations

The cross-sectional and longitudinal study had a relatively small sample size. Furthermore, the longitudinal study was limited by an intervention with very low calorie intake of 800 kcal per day.

6 Conclusion

6.1 Cross-sectional Study

The cross-sectional study allowed further insights into the association of different adipose tissue compartments. The liver as the central metabolic organ showed connections not only with the SAT and VAT volumes, but also with the unsaturation profile of the SAT. Thus, adipose tissue dysfunction, which is reflected in the unsaturation profile, may have a close connection with the liver fat content. Patient care can potentially benefit from this knowledge with regard to individual lifestyle interventions and appropriate treatments.

6.2 Longitudinal Study

Bone marrow showed a distinct change after the intervention in obese women. Changes in bone marrow were much smaller than in liver fat, SAT, VAT, and serum lipids. This was connected to fat distribution before the intervention, especially a higher SAT volume led to an increase in bone marrow fat. This specifically means that bone health could be affected in a negative way by such an intervention (Cordes et al., 2015).

7 Summary/ Abstract/ Zusammenfassung

7.1 Summary

Title: Cross-sectional and longitudinal MR-based evaluation of fat depots in subjects with obesity and risk factors for type 2 diabetes mellitus

Purpose: The purpose of the cross-sectional study was to investigate the metabolic associations between the liver fat, VAT (Visceral Adipose Tissue), SAT (Subcutaneous Adipose Tissue), bone marrow fat fraction (BMFF) and blood parameters in prediabetic subjects. The longitudinal study examined changes of composition and volumes of fat depots during a strict calorie reduced diet for a four-week period.

Materials and Methods: In the cross-sectional study 63 subjects were included (35 female and 28 male), who were classified as prediabetic. For the longitudinal study twenty obese women (BMI 34.9 ± 3.8 kg/m²) were recruited. Both studies included the measurement of blood fat values and anthropometric values. MR-examinations were performed in order to determine SAT and VAT volume as well as liver and bone marrow fat content.

Results: In the cross-sectional study, gender differences were only found for the VAT volume, which was greater in male subjects ($p = 0.032$). A strong correlation was found for the liver fat with the fasting insulin levels ($r = 0.664$), whereas it correlated moderately with SAT ($r = 0.505$) and VAT volumes ($r = 0.395$), weight ($r = 0.390$) and hip circumference ($r = 0.427$). The unsaturation of SAT correlated negatively with liver fat ($r = -0.53$, $p = 0.02$).

The longitudinal study demonstrated the greatest reduction of fat in the liver (-40.3%), followed by VAT (-15.1%), serum lipids (-12.6 - 14.5 %) and SAT volume (-8.5 %) after the calorie restriction. The BMFF did not change significantly, but showed a positive connection with the SAT volume ($r = 0.489$) and a negative connection with the NAT ($r = -0.493$) before the dietary intervention.

Conclusions: Results from the cross-sectional study showed the liver as a central metabolic organ which is not only connected with adipose tissue dysfunction, but also with unsaturation of the SAT. The longitudinal study demonstrated that BMFF behaves distinct from SAT and VAT volume, liver fat fraction or serum lipids.

7.2 Zusammenfassung

Titel: Querschnitts- und Längsschnittstudien zur MR-basierten Analyse von Fettdepots bei Patienten mit Adipositas und Risikofaktoren für Typ 2 Diabetes

Zielsetzung: Ziel der Querschnittsstudie war es die metabolische Verbindung zwischen der Leber, viszeralem Fettgewebe, subkutanem Fettgewebe, Knochenmarksfett und Blutwerten zu untersuchen. Die Längsschnittstudie konzentrierte sich auf die Auswirkung auf Fettvolumen- und Zusammensetzung während einer vier-wöchigen Kalorienrestriktion (800kcal/d).

Material und Methoden: In der Querschnittsstudie nahmen 63 als prädiabetisch klassifizierte Teilnehmer teil (35 Frauen und 28 Männer). Für die Längsschnittstudie wurden 20 übergewichtige Frauen rekrutiert (BMI 34.9 ± 3.8 kg/m^2). Zu beiden Studien gehörten sowohl Blutwertmessungen als auch anthropometrische Messungen. MR-Untersuchungen wurden durchgeführt, um subkutanes und viszerales Fettgewebe zu messen sowie Leber- und Knochenmarksfett zu bestimmen.

Ergebnisse: Die Querschnittsstudie konnte signifikante Unterschiede zwischen Männern und Frauen nur für das viszerale Fettgewebe zeigen, welches bei Männern größer war ($p = 0.032$). Eine starke Korrelation wurde für das Leberfett mit dem Nüchtern-Insulinspiegel gefunden ($r = 0.664$). Es korrelierte hingegen moderat mit dem subkutanen Fettgewebe ($r = 0.505$), dem viszeralen Fettgewebe ($r = 0.395$), dem Gewicht ($r = 0.390$) und dem Hüftumfang ($r = 0.427$). Der Anteil ungesättigter Fettsäuren im subkutanen Fettgewebe und das Leberfett korrelierten negativ miteinander ($r = -0.530$).

Die Längsschnittstudie zeigte, dass während der Diätintervention viel Fett abgebaut werden konnte. Am meisten in der Leber (-40.3%), danach im viszeralen Fett (-15.1%), den Blutfetten (-12.6 bis 14.5%) und dem subkutanen Fett (-8.5%). Das Knochenmarksfett hingegen änderte sich nicht statistisch signifikant, zeigte aber eine Abhängigkeit von der Fettverteilung zu Beginn der Studie. Hohes subkutanes Fettgewebe zu Beginn der Studie führte zu einem Anstieg des Knochenmarksfettes ($r = 0.489$). Ein hoher Anteil an Nicht-Fettgewebe (Muskeln, Wasser, Organe) hingegen führte zu einer Reduktion im Knochenmarksfett ($r = -0.493$).

Schlussfolgerungen: Aus der Querschnittsstudie lässt sich schließen, dass die Leber mit ihrer Rolle als zentrales metabolisches Organ nicht nur mit Fehlfunktionen und Vergrößerungen der Fettgewebe verknüpft ist, sondern auch mit dem Anteil von ungesättigten Fettsäuren im subkutanen Fett.

Die Längsschnittstudie zeigte, dass Knochenmarksfett sich anders als die abdominellen Fettgewebe und Blutfettwerte verhält.

8 References

Baek, K., & Bloomfield, S. A. (2012a). Blocking beta-adrenergic signaling attenuates reductions in circulating leptin, cancellous bone mass, and marrow adiposity seen with dietary energy restriction. *Journal of Applied Physiology, 113*(11), 1792-1801. doi:10.1152/japplphysiol.00187.2012

Baek, K., & Bloomfield, S. A. (2012b). Blocking beta-adrenergic signaling attenuates reductions in circulating leptin, cancellous bone mass, and marrow adiposity seen with dietary energy restriction. *J Appl Physiol (1985), 113*(11), 1792-1801. doi:10.1152/japplphysiol.00187.2012

Barcenilla-Wong, A. L., Chen, J. S., Cross, M. J., & March, L. M. (2015). The Impact of Fracture Incidence on Health Related Quality of Life among Community-Based Postmenopausal Women. *J Osteoporos, 2015*, 717914. doi:10.1155/2015/717914

Baum, T., Cordes, C., Dieckmeyer, M., Ruschke, S., Franz, D., Hauner, H., Kirschke, J. S., & Karampinos, D. C. (2016). MR-based assessment of body fat distribution and characteristics. *Eur J Radiol, 85*(8), 1512-1518. doi:10.1016/j.ejrad.2016.02.013

Baum, T., Yap, S. P., Karampinos, D. C., Nardo, L., Kuo, D., Burghardt, A. J., Masharani, U. B., Schwartz, A. V., Li, X., & Link, T. M. (2012). Does vertebral bone marrow fat content correlate with abdominal adipose tissue, lumbar spine bone mineral density, and blood biomarkers in women with type 2 diabetes mellitus? *J Magn Reson Imaging, 35*(1), 117-124. doi:10.1002/jmri.22757

Bingolbali, A., Fallone, B. G., & Yahya, A. (2015). Comparison of optimized long echo time STEAM and PRESS proton MR spectroscopy of lipid olefinic protons at 3 Tesla. *J Magn Reson Imaging, 41*(2), 481-486. doi:10.1002/jmri.24532

Bleibler, F., Rapp, K., Jaensch, A., Becker, C., & Konig, H. H. (2014). Expected lifetime numbers and costs of fractures in postmenopausal women with and without osteoporosis in Germany: a discrete event simulation model. *BMC Health Serv Res, 14*(284), 284. doi:10.1186/1472-6963-14-284

Borga, M., Thomas, E. L., Romu, T., Rosander, J., Fitzpatrick, J., Dahlqvist Leinhard, O., & Bell, J. D. (2015). Validation of a fast method for quantification of intra-abdominal and subcutaneous adipose tissue for large-scale human studies. *NMR Biomed, 28*(12), 1747-1753. doi:10.1002/nbm.3432

Bosy‐Westphal, A., Later, W., Schautz, B., Lagerpusch, M., Goele, K., Heller, M., Glüer, C. C., & Müller, M. J. (2011). Impact of intra‐and extra‐osseous soft tissue composition on changes in bone mineral density with weight loss and regain. *Obesity, 19*(7), 1503-1510.

Bredella, M. A., Fazeli, P. K., Daley, S. M., Miller, K. K., Rosen, C. J., Klibanski, A., & Torriani, M. (2014). Marrow fat composition in anorexia nervosa. *Bone, 66*, 199-204. doi:10.1016/j.bone.2014.06.014

Bredella, M. A., Fazeli, P. K., Miller, K. K., Misra, M., Torriani, M., Thomas, B. J., Ghomi, R. H., Rosen, C. J., & Klibanski, A. (2009). Increased bone marrow fat in anorexia nervosa. *J Clin Endocrinol Metab, 94*(6), 2129-2136. doi:10.1210/jc.2008-2532

Bredella, M. A., Gill, C. M., Gerweck, A. V., Landa, M. G., Kumar, V., Daley, S. M., Torriani, M., & Miller, K. K. (2013). Ectopic and serum lipid levels are positively associated with bone marrow fat in obesity. *Radiology, 269*(2), 534-541.

Bredella, M. A., Torriani, M., Ghomi, R. H., Thomas, B. J., Brick, D. J., Gerweck, A. V., Rosen, C. J., Klibanski, A., & Miller, K. K. (2011). Vertebral bone marrow fat is positively associated with visceral fat and inversely associated with IGF-1 in obese women. *Obesity (Silver Spring), 19*(1), 49-53. doi:10.1038/oby.2010.106

Chaston, T. B., & Dixon, J. B. (2008). Factors associated with percent change in visceral versus subcutaneous abdominal fat during weight loss: findings from a systematic review. *Int J Obes (Lond), 32*(4), 619-628. doi:10.1038/sj.ijo.0803761

Cohen, A., Shen, W., Dempster, D. W., Zhou, H., Recker, R. R., Lappe, J. M., Kepley, A., Kamanda-Kosseh, M., Bucovsky, M., Stein, E. M., Nickolas, T. L., & Shane, E. (2015). Marrow adiposity assessed on transiliac crest biopsy samples correlates with noninvasive measurement of marrow adiposity by proton magnetic resonance spectroscopy ((1)H-MRS) at the spine but not the femur. *Osteoporos Int, 26*(10), 2471-2478. doi:10.1007/s00198-015-3161-7

Cordes, C., Dieckmeyer, M., Ott, B., Shen, J., Ruschke, S., Settles, M., Eichhorn, C., Bauer, J. S., Kooijman, H., Rummeny, E. J., Skurk, T., Baum, T., Hauner, H., & Karampinos, D. C. (2015). MR-detected changes in liver fat, abdominal fat, and vertebral bone marrow fat after a four-week calorie restriction in obese women. *J Magn Reson Imaging, 42*(5), 1272-1280. doi:10.1002/jmri.24908

Cowin, G. J., Jonsson, J. R., Bauer, J. D., Ash, S., Ali, A., Osland, E. J., Purdie, D. M., Clouston, A. D., Powell, E. E., & Galloway, G. J. (2008). Magnetic resonance imaging and spectroscopy for monitoring liver steatosis. *Journal of Magnetic Resonance Imaging, 28*(4), 937-945.

Deutsches Institut für Ernährungsforschung Potsdam-Rehbrücke (DIfE). (2014). Deutscher Diabetes Risiko Test.

Deutsches Zentrum für Diabetesforschung. (2017). Prädiabetes Lebensstil-Interventions-Studie (PLIS). Retrieved from https://www.dzd-ev.de/forschung/bereiche/klinische-studien/index.html

Devlin, M. J., Cloutier, A. M., Thomas, N. A., Panus, D. A., Lotinun, S., Pinz, I., Baron, R., Rosen, C. J., & Bouxsein, M. L. (2010). Caloric restriction leads to high marrow adiposity and low bone mass in growing mice. *J Bone Miner Res, 25*(9), 2078-2088. doi:10.1002/jbmr.82

Donald W. McRobbie, E. A. M., Martin J. Graves, Martin R. Prince. (2006). MRI from Picture to Proton. *2*, 32, 93, 310-313.

Ecklund, K., Vajapeyam, S., Mulkern, R. V., Feldman, H. A., O'Donnell, J. M., DiVasta, A. D., & Gordon, C. M. (2017). Bone marrow fat content in 70 adolescent girls with anorexia nervosa: Magnetic resonance imaging and magnetic resonance spectroscopy assessment. *Pediatric Radiology*, 1-11.

Else Kröner-Fresenius Zentrum für Ernährungsmedizin der Technischen Universität München. (2017). PLIS - Prädiabetes Lebensstil Interventionsstudie. Retrieved from http://www.kem.wzw.tum.de/index.php?id=62

Ermetici, F., Briganti, S., Delnevo, A., Cannaò, P., Di Leo, G., Benedini, S., Terruzzi, I., Sardanelli, F., & Luzi, L. (2017). Bone marrow fat contributes to insulin sensitivity and adiponectin secretion in premenopausal women. *Endocrine*, 1-9.

Fox, C. S., Massaro, J. M., Hoffmann, U., Pou, K. M., Maurovich-Horvat, P., Liu, C. Y., Vasan, R. S., Murabito, J. M., Meigs, J. B., Cupples, L. A., D'Agostino, R. B., Sr., & O'Donnell, C. J. (2007). Abdominal visceral and subcutaneous adipose tissue compartments: association with metabolic risk factors in the Framingham Heart Study. *Circulation, 116*(1), 39-48. doi:10.1161/CIRCULATIONAHA.106.675355

Griffith, J. F., Yeung, D. K., Antonio, G. E., Lee, F. K., Hong, A. W., Wong, S. Y., Lau, E. M., & Leung, P. C. (2005). Vertebral bone mineral density, marrow perfusion, and fat content in healthy men and men with osteoporosis: dynamic contrast-enhanced MR imaging and MR spectroscopy. *Radiology, 236*(3), 945-951. doi:10.1148/radiol.2363041425

Griffith, J. F., Yeung, D. K., Antonio, G. E., Wong, S. Y., Kwok, T. C., Woo, J., & Leung, P. C. (2006). Vertebral marrow fat content and diffusion and perfusion indexes in

women with varying bone density: MR evaluation. *Radiology, 241*(3), 831-838. doi:10.1148/radiol.2413051858

Griffith, J. F., Yeung, D. K., Chow, S. K., Leung, J. C., & Leung, P. C. (2009). Reproducibility of MR perfusion and (1)H spectroscopy of bone marrow. *J Magn Reson Imaging, 29*(6), 1438-1442. doi:10.1002/jmri.21765

Hernlund, E., Svedbom, A., Ivergard, M., Compston, J., Cooper, C., Stenmark, J., McCloskey, E. V., Jonsson, B., & Kanis, J. A. (2013). Osteoporosis in the European Union: medical management, epidemiology and economic burden. A report prepared in collaboration with the International Osteoporosis Foundation (IOF) and the European Federation of Pharmaceutical Industry Associations (EFPIA). *Arch Osteoporos, 8*(136), 136. doi:10.1007/s11657-013-0136-1

Hu, H. H., Nayak, K. S., & Goran, M. I. (2011). Assessment of abdominal adipose tissue and organ fat content by magnetic resonance imaging. *Obes Rev, 12*(5), e504-515. doi:10.1111/j.1467-789X.2010.00824.x

Hu, M., Sheng, J., Kang, Z., Zou, L., Guo, J., & Sun, P. (2014). Magnetic resonance imaging and dual energy X-ray absorptiometry of the lumbar spine in professional wrestlers and untrained men. *J Sports Med Phys Fitness, 54*(4), 505-510.

International Diabetes Federation. Retrieved from https://www.idf.org/e-library/consensus-statements/60-idfconsensus-worldwide-definitionof-the-metabolic-syndrome.html

Kantartzis, K., Machann, J., Schick, F., Rittig, K., Machicao, F., Fritsche, A., Häring, H.-U., & Stefan, N. (2011). Effects of a lifestyle intervention in metabolically benign and malign obesity. *Diabetologia, 54*(4), 864-868.

Karampinos, D. C., Ruschke, S., Gordijenko, O., Grande Garcia, E., Kooijman, H., Burgkart, R., Rummeny, E. J., Bauer, J. S., & Baum, T. (2015). Association of MRS-Based Vertebral Bone Marrow Fat Fraction with Bone Strength in a Human In Vitro Model. *J Osteoporos, 2015*, 152349. doi:10.1155/2015/152349

Kim, T. Y., Schwartz, A. V., Li, X., Xu, K., Black, D. M., Petrenko, D. M., Stewart, L., Rogers, S. J., Posselt, A. M., Carter, J. T., Shoback, D. M., & Schafer, A. L. (2017). Bone Marrow Fat Changes After Gastric Bypass Surgery Are Associated With Loss of Bone Mass. *J Bone Miner Res*. doi:10.1002/jbmr.3212

Kotronen, A., Juurinen, L., Hakkarainen, A., Westerbacka, J., Corner, A., Bergholm, R., & Yki-Jarvinen, H. (2008). Liver fat is increased in type 2 diabetic patients and underestimated by serum alanine aminotransferase compared with equally obese nondiabetic subjects. *Diabetes care, 31*(1), 165-169. doi:10.2337/dc07-1463

Kugel, H., Jung, C., Schulte, O., & Heindel, W. (2001). Age- and sex-specific differences in the 1H-spectrum of vertebral bone marrow. *J Magn Reson Imaging, 13*(2), 263-268.

Lebovitz, H. E., & Banerji, M. A. (2005). Point: Visceral Adiposity Is Causally Related to Insulin Resistance. *Diabetes care, 28*(9), 2322-2325. doi:10.2337/diacare.28.9.2322

Lemieux, S., Prud'homme, D., Bouchard, C., Tremblay, A., & Després, J.-P. (1993). Sex differences in the relation of visceral adipose tissue accumulation to total body fatness. *The American journal of clinical nutrition, 58*(4), 463-467.

Li, X., Kuo, D., Schafer, A. L., Porzig, A., Link, T. M., Black, D., & Schwartz, A. V. (2011). Quantification of vertebral bone marrow fat content using 3 Tesla MR spectroscopy: reproducibility, vertebral variation, and applications in osteoporosis. *J Magn Reson Imaging, 33*(4), 974-979. doi:10.1002/jmri.22489

Lomonaco, R., Ortiz‐Lopez, C., Orsak, B., Webb, A., Hardies, J., Darland, C., Finch, J., Gastaldelli, A., Harrison, S., & Tio, F. (2012). Effect of adipose tissue insulin resistance on metabolic parameters and liver histology in obese patients with nonalcoholic fatty liver disease. *Hepatology, 55*(5), 1389-1397.

Lundbom, J., Hakkarainen, A., Soderlund, S., Westerbacka, J., Lundbom, N., & Taskinen, M. R. (2011). Long-TE 1H MRS suggests that liver fat is more saturated than subcutaneous and visceral fat. *NMR Biomed, 24*(3), 238-245. doi:10.1002/nbm.1580

Machann, J., Stefan, N., Schabel, C., Schleicher, E., Fritsche, A., Würslin, C., Häring, H. U., Claussen, C. D., & Schick, F. (2013). Fraction of unsaturated fatty acids in visceral adipose tissue (VAT) is lower in subjects with high total VAT volume–a combined 1H MRS and volumetric MRI study in male subjects. *NMR in Biomedicine, 26*(2), 232-236.

Mierisova, S., & Ala-Korpela, M. (2001). MR spectroscopy quantitation: a review of frequency domain methods. *NMR Biomed, 14*(4), 247-259.

Nakamura, T., Tokunaga, K., Shimomura, I., Nishida, M., Yoshida, S., Kotani, K., Islam, A. H. M. W., Keno, Y., Kobatake, T., Nagai, Y., Fujioka, S., Tarui, S., & Matsuzawa, Y. (1994). Contribution of visceral fat accumulation to the development of coronary artery disease in non-obese men. *Atherosclerosis, 107*(2), 239-246. doi:10.1016/0021-9150(94)90025-6

National Institute of Diabetes and Digestive and Kidney Diseases. Overweight and Obesity Statistics. Retrieved from http://www.niddk.nih.gov/health-information/health-statistics/Pages/overweight-obesity-statistics.aspx

Ojanen, X., Borra, R. J., Havu, M., Cheng, S. M., Parkkola, R., Nuutila, P., Alen, M., & Cheng, S. (2014). Comparison of vertebral bone marrow fat assessed by 1H MRS and inphase and out-of-phase MRI among family members. *Osteoporos Int, 25*(2), 653-662. doi:10.1007/s00198-013-2472-9

Paccou, J., Hardouin, P., Cotten, A., Penel, G., & Cortet, B. (2015). The Role of Bone Marrow Fat in Skeletal Health: Usefulness and Perspectives for Clinicians. *J Clin Endocrinol Metab, 100*(10), 3613-3621. doi:10.1210/jc.2015-2338

Pansini, V. M., Monnet, A., Salleron, J., Penel, G., Migaud, H., & Cotten, A. (2012). Reproducibility of 1H MR spectroscopy of hip bone marrow at 3 Tesla. *J Magn Reson Imaging, 36*(6), 1445-1449. doi:10.1002/jmri.23783

Rummeny, E. J., Reimer, P., & Heindel, W. (2006). Ganzkoerper-MR-Tomographie. *2*, 192.

Ruschke, S., Kienberger, H., Baum, T., Kooijman, H., Settles, M., Haase, A., Rychlik, M., Rummeny, E. J., & Karampinos, D. C. (2016). Diffusion-weighted stimulated echo acquisition mode (DW-STEAM) MR spectroscopy to measure fat unsaturation in regions with low proton-density fat fraction. *Magn Reson Med, 75*(1), 32-41. doi:10.1002/mrm.25578

Sadie-Van Gijsen, H., Hough, F. S., & Ferris, W. F. (2013). Determinants of bone marrow adiposity: the modulation of peroxisome proliferator-activated receptor-gamma2 activity as a central mechanism. *Bone, 56*(2), 255-265. doi:10.1016/j.bone.2013.06.016

Schafer, A. L., Li, X., Schwartz, A. V., Tufts, L. S., Wheeler, A. L., Grunfeld, C., Stewart, L., Rogers, S. J., Carter, J. T., Posselt, A. M., Black, D. M., & Shoback, D. M. (2015). Changes in vertebral bone marrow fat and bone mass after gastric bypass surgery: A pilot study. *Bone, 74*, 140-145. doi:10.1016/j.bone.2015.01.010

Schreiner, P. J., Terry, J. G., Evans, G. W., Hinson, W. H., Crouse, J. R., 3rd, & Heiss, G. (1996). Sex-specific associations of magnetic resonance imaging-derived intra-abdominal and subcutaneous fat areas with conventional anthropometric indices. The Atherosclerosis Risk in Communities Study. *Am J Epidemiol, 144*(4), 335-345.

Shen W, C. J., Punyanitya M, Shapses S, Heshka S, Heymsfield SB. (2007). MRI-measured bone marrow adipose tissue: changes during weight loss and its relationship with DXA-measured bone mineral. *The FASEB Journal, 21*, 831. doi:10.1096/fj.1530-6860

Shen, W., Gong, X., Weiss, J., & Jin, Y. (2013). Comparison among T1-weighted magnetic resonance imaging, modified dixon method, and magnetic resonance spectroscopy in measuring bone marrow fat. *J Obes, 2013*, 298675. doi:10.1155/2013/298675

Shen, W., Wang, Z., Punyanita, M., Lei, J., Sinav, A., Kral, J. G., Imielinska, C., Ross, R., & Heymsfield, S. B. (2003). Adipose tissue quantification by imaging methods: a proposed classification. *Obes Res, 11*(1), 5-16. doi:10.1038/oby.2003.3

Straub, B. K., & Schirmacher, P. (2010). Pathology and biopsy assessment of non-alcoholic fatty liver disease. *Dig Dis, 28*(1), 197-202. doi:10.1159/000282086

Taksali, S. E., Caprio, S., Dziura, J., Dufour, S., Calí, A. M., Goodman, T. R., Papademetris, X., Burgert, T. S., Pierpont, B. M., & Savoye, M. (2008). High visceral and low abdominal subcutaneous fat stores in the obese adolescent. *Diabetes, 57*(2), 367-371.

Thoma, C., Day, C. P., & Trenell, M. I. (2012). Lifestyle interventions for the treatment of non-alcoholic fatty liver disease in adults: a systematic review. *J Hepatol, 56*(1), 255-266. doi:10.1016/j.jhep.2011.06.010

Vitola, B. E., Deivanayagam, S., Stein, R. I., Mohammed, B. S., Magkos, F., Kirk, E. P., & Klein, S. (2009). Weight loss reduces liver fat and improves hepatic and skeletal muscle insulin sensitivity in obese adolescents. *Obesity, 17*(9), 1744-1748.

Westerbacka, J., Corner, A., Tiikkainen, M., Tamminen, M., Vehkavaara, S., Hakkinen, A. M., Fredriksson, J., & Yki-Jarvinen, H. (2004). Women and men have similar amounts of liver and intra-abdominal fat, despite more subcutaneous fat in women: implications for sex differences in markers of cardiovascular risk. *Diabetologia, 47*(8), 1360-1369. doi:10.1007/s00125-004-1460-1

World Gastroenterology Organisation. (2012). Retrieved from http://www.worldgastroenterology.org/guidelines/global-guidelines/nafld-nash/nafld-nash-english

World Health Organisation. (2016a). Diabetes. Retrieved from http://www.who.int/mediacentre/factsheets/fs312/en/

World Health Organisation. (2016b). Obesity and Overweight. Retrieved from http://www.who.int/mediacentre/factsheets/fs311/en/

Wren, T. A., Chung, S. A., Dorey, F. J., Bluml, S., Adams, G. B., & Gilsanz, V. (2011). Bone marrow fat is inversely related to cortical bone in young and old subjects. *J Clin Endocrinol Metab, 96*(3), 782-786. doi:10.1210/jc.2010-1922

Yeung, D. K., Griffith, J. F., Antonio, G. E., Lee, F. K., Woo, J., & Leung, P. C. (2005). Osteoporosis is associated with increased marrow fat content and decreased marrow fat unsaturation: a proton MR spectroscopy study. *J Magn Reson Imaging, 22*(2), 279-285. doi:10.1002/jmri.20367

Yu, N., Wolfson, T., Middleton, M., Hamilton, G., Gamst, A., Angeles, J., Schwimmer, J., & Sirlin, C. (2017). Bone marrow fat content is correlated with hepatic fat content in paediatric non-alcoholic fatty liver disease. *Clinical radiology, 72*(5), 425. e429-425. e414.

9 Appendix

9.1 List of Figures

9.2 List of Tables

9.3 Published journal papers:

The present work resulted into two first-authored journal publications and contributed to four co-authored journal publications.

1. ***C. Cordes***, M. Dieckmeyer, B. Ott, J. Shen, S. Ruschke, M. Settles, Eichhorn, C., Bauer, J. S., Kooijman, H., Rummeny, E. J., Skurk, T., Baum, T., Hauner, H., Karampinos, D. C.., "MR-detected changes in liver fat, abdominal fat, and vertebral bone marrow fat after a four-week calorie restriction in obese women," J Magn Reson Imaging, vol. 42, pp. 1272-80, Nov 2015. Orginal article
2. ***C. Cordes***, T. Baum, M. Dieckmeyer, S. Ruschke, M. N. Diefenbach, H. Hauner, Kirschke, J. S., Karampinos, D. C.., "MR-Based Assessment of Bone Marrow Fat in Osteoporosis, Diabetes, and Obesity," Frontiers in Endocrinology, vol. 7, 2016. Review
3. T. Baum, ***C. Cordes***, M. Dieckmeyer, S. Ruschke, D. Franz, H. Hauner, Kirschke, J. S., Karampinos, D. C.., "MR-based assessment of body fat distribution and characteristics," Eur J Radiol, vol. 85, pp. 1512-8, Aug 2016. Review
4. M. Dieckmeyer, S. Ruschke, ***C. Cordes***, S. P. Yap, H. Kooijman, H. Hauner, Rummeny, E. J., Bauer, J. S., Baum, T., Karampinos, D. C.., "The need for T(2) correction on MRS-based vertebral bone marrow fat quantification: implications for bone marrow fat fraction age dependence," NMR Biomed, vol. 28, pp. 432-9, Apr 2015. Orginal article
5. J. Shen, T. Baum, ***C. Cordes***, B. Ott, T. Skurk, H. Kooijman, Rummeny, E. J., Hauner, H., Menze, B. H., Karampinos, D. C., "Automatic segmentation of abdominal organs and adipose tissue compartments in water-fat MRI: Application to weight-loss in obesity," European Journal of Radiology, vol. 85, pp 1613-1621, 2016. Original article
6. T. Baum, S. Inhuber, M. Dieckmeyer, ***C. Cordes***, S. Ruschke, E. Klupp, Jungmann, P. M., Farlock, R., Eggers, H., Kooijman, H.., "Association of Quadriceps Muscle Fat With Isometric Strength Measurements in Healthy Males Using Chemical Shift Encoding-Based Water-Fat Magnetic Resonance Imaging," Journal of computer assisted tomography, vol. 40, p. 447, 2016. Technical Note

9.4 Published conference abstracts:

Part of the present work was presented in two first-authored conference abstracts in International Conference Proceedings:

1. **C. Cordes**, M. Dieckmeyer, B. Ott, J. Shen, S. Ruschke, M. Settles et al., ”Bone marrow fat behaves differently from abdominal fat, liver fat and serum lipids after a four-week calorie restriction in obese women”, ISMRM 2015 Abstract #4117
2. **C. Cordes**, T. Baum, J. Clavel, S. Ruschke, M. Dieckmeyer, D. Franz et al., “Subcutaneous fat unsaturation is negatively associated with liver fat fraction”, ISMRM 2016 Abstract #3913

9.5 Acknowledgement

I would not have been able to create this thesis without the support from several people: Especially I would like to thank my supervisors Prof. Dr. med. Ernst J. Rummeny, PD Dr. med. Thomas Baum and PD Dr. Dimitrios Karampinos, Ph.D.. They introduced me into scientific work, the technical background of MR, helped a lot with the statistical analysis and where always available for questions. I would like to thank the whole research group Body Magnetic Resonance Imaging from the Department of Diagnostic and Interventional Radiology, Technische Universität München.